Journal of Hydraulic Structures
J. Hydraul. Struct., 2021; 7(4):58-75
DOI: 10.22055/jhs.2022.40233.1203

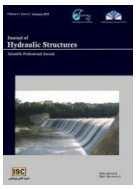

OPEN ACCESS

Experimental investigation on the characteristics of hydraulic jump in expanding channels with a water jet injection system

Shokoofeh Sharoonizadeh[1]
Javad Ahadiyan[2]
Manoochehr Fathi Moghadam[1]
Mohsen Sajjadi[1]
Mario Di Bacco[3]

Abstract

The high flow velocity downstream of weirs and gates can cause the destruction of erosive beds in rivers or even non-erosive channels. To reduce the flow's kinetic energy, structures are needed to consume this energy. Expansion basins are often used downstream of structures such as weirs, gates, and chutes to increase energy dissipation in hydraulic jumps. Various methods are used to stabilize asymmetric hydraulic jumps in abrupt expanding channels. In this study, the interaction of multiple submerged water jet injection systems with S-type hydraulic jump for stabilizing and stabilizing the hydraulic jump was investigated. The different configurations of the jet system were tested with Froude numbers 7.4, 8.7, and 9.5, and finally, three optimal configurations were selected as configurations 1, 2, and 3. In order to investigate the performance of the jet injection system under other hydraulic boundary conditions, flow velocities downstream of the jet system were measured for three optimal configurations with different depths of the tailwater. Comparison of the results of using a water jet injection system with S-type hydraulic jump showed that the energy and momentum correction coefficients in all different configurations were significantly reduced. The highest relative energy loss was observed in configuration 3, equal to 68.42%. The results showed a good performance of the jet injection system in stabilizing the asymmetric hydraulic jump S and reducing the length of the stilling basin.

Keywords: Asymmetric Hydraulic Jump, Water Jet Injection System, Expanding Channels, Energy Loss, Stilling Basin.

Received: 07 February 2022; Accepted: 10 March 2022

[1] Dept. of Hydraulic Structures, College of Water and Environmental Engineering, Shahid Chamran University of Ahvaz.
[2] Dept. of Hydraulic Structures, College of Water and Environmental Engineering, Shahid Chamran University of Ahvaz. E-mail: j.ahadiyan@scu.ac.ir **(Corresponding author)**
[3] Dept. of Civil, Environmental and Architectural Engineering, University of L'Aquila, Via G. Gronchi, 18, 67100 L'Aquila, Italy

1. Introduction

In hydraulic structures, the hydraulic jump is used as an energy dissipator downstream of a stilling basin [1]. It is mainly intended to reduce or eliminate the flow erosion at the end of the stilling basin. To this end, it dissipates a large amount of kinetic energy at a high flow rate into the stilling basin. The common techniques to achieve this goal include baffle piers, end sills, and chute blocks [2]. Many researchers have studied these methods for reducing downstream depth, increasing energy loss, and shortening the basin length required for a design discharge (e.g., Rajaratnam, [3], Basco and Adams [4], Rajaratnam and Murahari [5], Peterka [6], Ohtsu et al. [7], Hager [8], Thompson and Kilgore [9], Habibzadeh et al. [10], Abdelhaleem [11], Aal et al. [12]). In practical cases where the tailwater depth is very low, the classical jump cannot be created even using the fittings, and it is not possible to drill the basin floor. The channel expansion can be a practical solution for energy dissipation [13]. However, in some cases, unwanted phenomena, such as instability and asymmetric flows, may occur in specific tailwater conditions [14]. The downstream water level greatly influences the formation of hydraulic jump flow pattern in an abrupt expansion section. Therefore, according to the position of the jump toe, which is dependent on the tailwater depth, in an abrupt expansion section, four types of jumps are formed: Repelled Jump, Spatial Jump, Transitional Jump, and Classical jump. The type S-jump investigated in this study occurs when the jump toe is located between abrupt section change and the point where the transverse waves intersect the downstream channel. This type of jump is more like a jet and is asymmetric. The direction of inclination to one side of the channel wall is completely random and may incline to the left or right. This asymmetric jump can be a stable or oscillation asymmetric [15].

Tharp [2] conducted a study to investigate the effect of injecting submerged water jets on the classical hydraulic jump. The experiments showed that the submerged jets at each angle tested tend to decrease the water specific energy released and the tailwater depth required for the formation of the jump, and showed a greater effect than the impulse-momentum principle. The submerged jets may be as effective as the stilling blocks in reducing the jump length. Varol et al. [16] investigated the effect of water jet in a horizontal channel with different flow rates on hydraulic jump characteristics. The experiments were carried out upstream at different Froude numbers ranging from 3.43 to 4.83 and five different water jet flow rates. Flow structure, roller length, water surface profile, and energy losses during the free hydraulic jump and the hydraulic jump with water jet were examined and compared. Wali [17] determined the kinetic energy and momentum Correction coefficients experimentally in a trapezoidal irrigation channel. Khalili Shayan and Farhoudi [18] theoretically investigated the stability of free hydraulic jump on adverse stilling basins. Scorzini et al. [14] investigated the S- and T-type jump control using a crossbeam system as an energy dissipator in the abrupt expansion channels. The results showed that using the dissipator improves the flow patterns in the tailwater channel, and the most important parameters affecting the performance are determined by system orientation and distance of the beams. Helal et al. [19] numerically investigated the performance of bed water jets in submerged hydraulic jumps. They simulated the submerged hydraulic jumps with and without bed water jets according to the main flow rate at the initial Froude numbers between 2.2 and 6.06 using a range of the jet relative discharges from 0 to 30%. The simulation results showed that the bed water jets improved the efficiency of submerged hydraulic jumps by approximately 85.4% and decreased the submerged jump length by about 59% compared to the system without the jet. Hajialigol et al. [20] investigated the flow patterns in Abruptly Expanding Channels using cross beams to control the effect of asymmetric jumps. Sharonizadeh et al. [21] proposed a new energy dissipator in the form of a multi-submersible water jet

injection system located at the bottom of the channel and in the opposite direction of the flow direction for the stability of the S-jump. The proposed dissipator consists of a pipe with some holes, which was used in the abruptly expanding channels. The main weakness of other jump control methods, such as baffle piers, namely the failure to withstand the damage from cavitation and floating debris, is less seen in this method.

By studying the researches, it can be concluded that the use of submersible jets causes energy consumption and affects other characteristics of hydraulic jump. It is possible to increase the passing flow using the submerged jet downstream of the weir on the bottom of the stilling basin for identical heads on the weir. Therefore, in the event of floods, it can prevent the creation of additional loads and cavitation on the weir. Also, this method can avoid submergence of the lands upstream of diversion dams by increasing the upstream water level. Therefore, in this research, the energy consuming performance proposed by Sharoonizadeh et al. [21] has been evaluated in more detail. The performance of this method has been evaluated after examining the flow symmetry, velocity distribution in the tailwater channel, and stability in different downstream conditions. Energy and momentum correction coefficients were developed for Froude numbers and different tailwater depths. Drag force, energy loss and jump length have also been studied.

2. Materials and methods

The experiments of this research were carried out in a flume in the hydraulic laboratory of the Faculty of Water Science Engineering in Shahid Chamran University of Ahvaz, Iran. Experimental design includes a horizontal rectangular channel with glass wall and metal floor, 12 m long, 1 m wide and 0.87 m deep, an upstream storage tank, 2.4 m long and 1 m wide, and an Ogee weir with 0.67 m wide and a height of 0.6 m and a vertical sluice gate at the end of the flume to control the depth of the tailwater. After the weir to create an abrupt expansion with a section opening ratio of 0.67 m, two boxes of plexiglass with 0.6 m length, 0.17 m width, and 0.3 m depth were installed on both sides of the cross-section of the flume. The water jet injection system also consisted of a 0.0317 m diameter PVC pipe, 1 m long across the width of the flume with holes 0.0095 m in diameter with equal distances of 0.085 m placed on the bottom of the flume. The pipe was connected on both sides by a 0.0317 m diameter PVC pipe to a 0.0508 m feed pipe. The inlet of this pipe was in the tank behind the weir. A pump provided the required discharges of this system. Also, to measure the discharges of this system, an electromagnetic flowmeter was used. Fig.1 shows the general plan of the laboratory flume used.

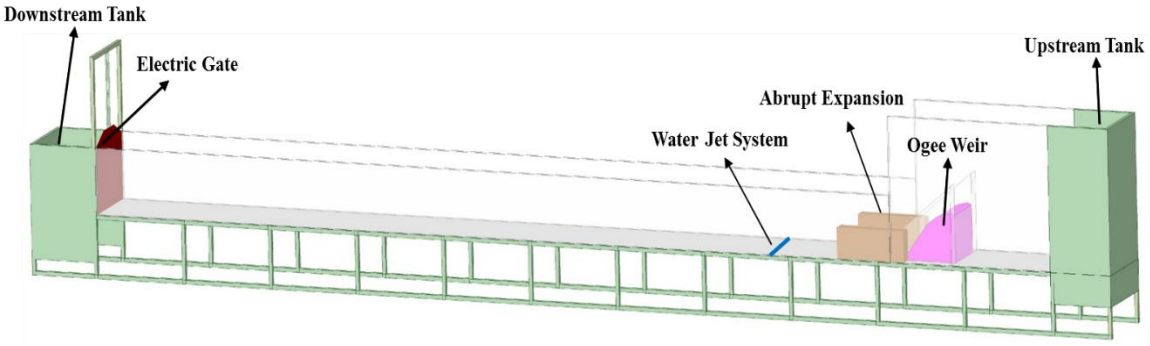

Figure 1. General plan of the laboratory flume

In the first phase of the experiments, the downstream conditions were identified to test the dissipator performance. In this way, the tailwater depth was checked by adjusting the end gate to form the S-type jump at each flow rate by bringing the jump toe to the edge of the expansion section. Therefore, the S-type jumps were formed by reaching the tailwater depth (hs) to 0.188, 0.148, and 0.110 m for the Froude numbers equal to 7.4, 8.7, and 9.5, respectively. The longitudinal velocities were measured at a constant height of 0.005 m from the channel bed for a time period of 30 seconds using a micro propeller velocity meter in 8 representatives cross-sections located 0.25, 0.50, 0.75, 1, 1.25, 1.5, 2.5, and 8 m after the abrupt expansion. In each section, nine measuring points were created along the channel axis at a distance of 0.1 m from each other. In the second phase of experiments, 54 experiments were performed using a water jet injection system for three fixed inlet flow rates and different configurations of the jet system [21]. The distance of the jet system from the section of abrupt expansion in the flume (P = 0.4, 0.6, and 0.8 m), the number of holes in the water jet injection system (n = 5, 7, and 9), and the flow rate of the jet (Qj = 0.0072 and 0.0081 m^3/s) were considered as variables in the configurations. For each tested configuration, after using the water jet injection system, the depth of the tailwater for each discharge was set equal to the depth of the control tailwater (the depth of the tailwater required for the S-jump in the first scenario). For this stage of experiments, longitudinal velocity measurements were performed in the control section located 0.5 m after the dissipator using a similar method previously described for the first stage. This stage of experiments aimed to investigate the effect of different variables on system performance and to find the best case that causes uniform and acceptable velocity distributions in the channel expansion section. The third phase of the experiments was aimed to investigate the behavior of the best performing configurations under other hydraulic boundary conditions, including the continuous change of downstream water level with the occurrence of S-type jump for different percentages of the tested tailwater depths.

In this experiment phase, the longitudinal velocity was measured in 5 control sections located 0.25, 0.5, 0.75, 1, and 2 m downstream of the dissipator end using the same method as the previous steps. In the last phase, the more detailed study of the velocity and flow pattern after the water jet injection system was performed using a three-dimensional electromagnetic velocity meter (JFE Advantech Co. ACM3-RS 3 axis, with an accuracy of _2% of true velocity) for the best configurations obtained from the results. In each section, 0.25, 0.5, 1, and 2 m after the water jet injection system, 9 points were measured in the flume width direction and 2-7 points in the flume depth direction, depending on the water depth, for a Froude number equal to 7.4 and different percentages of tailwater depth. In this study, the performance of different configurations of the water jet injection system was evaluated based on the parameters α_b and β_b for Froude numbers 7.4, 8.7, and 9.5. The parameters α_b and βb are the same value as the energy and momentum correction coefficients (Coriolis and Boussinesq coefficients) and are based on the general parameter, v_m. The parameters α_b and β_b provide information about the uniformity of flow and the average longitudinal velocity recorded in the measured sections near the channel bed [14] [21]. These parameters were defined at a measured height of 0.005 m from the channel bed, as follows:

$$\boldsymbol{\alpha_b} = \frac{\int_0^B \boldsymbol{v_b(x)^2}.|\boldsymbol{v_b(x)}|\boldsymbol{dx}}{\boldsymbol{B}.\boldsymbol{v_{m_b}^3}} \tag{1}$$

$$\boldsymbol{\beta_b} = \frac{\int_0^B \boldsymbol{v_b(x)}.|\boldsymbol{v_b(x)}|\boldsymbol{dx}}{\boldsymbol{B}.\boldsymbol{v_{mb}^2}} \tag{2}$$

Where in:
B: channel width, $v_b(x)$ is the near-bed longitudinal velocity across the section, and v_{mb} is the average value of $v_b(x)$. $\beta_b \cdot v^2_{mb}$ Provides information on the dynamic force of the flow (per unit height in the depth of measurement) and scouring potential, which is important in evaluating the performance of stilling basins in downstream of hydraulic structures. Also, kinetic energy (α) and momentum (β) correction coefficients in the total cross-section [1][17][22-25] using measured velocities with EMV velocity meter were calculated according to the equations (3) and (4) for four different depths of flow (0.75hs, 0.8hs, 0.9hs, hs).

$$\boldsymbol{\alpha} = \frac{\int_0^A \boldsymbol{v(x)^2, |v(x)| dA}}{\boldsymbol{v_m^3, A}} \tag{3}$$

$$\boldsymbol{\beta} = \frac{\int_0^A \boldsymbol{v(x), |v(x)| dA}}{\boldsymbol{v_m^2, A}} \tag{4}$$

Where in:
A: total flow cross-section, v (x): velocity profiles in the measured section and v_m: mean v (x). In this study, to check the uniformity of flow, energy, and momentum correction coefficients near the channel bed (α_b and β_b) and the total cross-section (α and β) were calculated by linear regression using MATLAB software.

3. Results and Discussion

In Fig. 2, the S-type jump (Fig. 2-a), the jump with the jet system in the flow path (in the off state) (Fig. 2-b), and also the stabilized form of the jump with the water jet injection system (in the on the state) (Fig. 2-c) is shown.

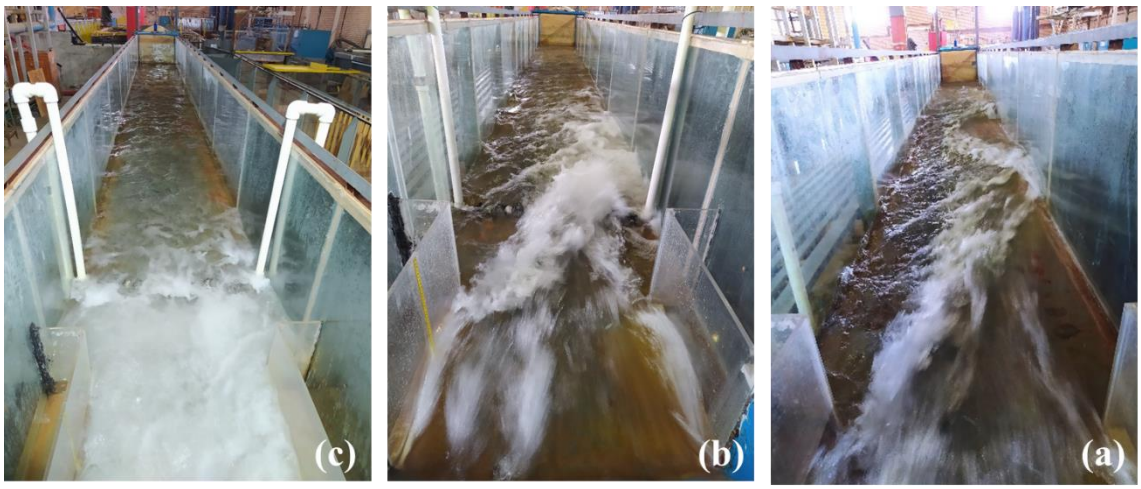

Figure 2. View of S-type jump (a), jump with the off jet system (b) and jump with the on jet system (c).

In the asymmetric jump of S-type, high local velocities were observed on the right side of the channel, where the main flow was concentrated, with negative values on the opposite side in the reverse flow region. As shown in Fig. 2-b, there is still an asymmetric mode of S-type jump

when the jet system is in the flow path. While by injecting a water jet into the jump, the asymmetric waves of S-type jump are eliminated, and the jump is stabilized. The values of β_b and α_b calculated at the measurement sections along the channel for asymmetric S-type jump and the position of the jet system in the flow path (in the off state) are shown in Fig. 3. In both cases, β_b was greater than 2 in most sections along the entire channel and reached about 3 downstream of the abrupt expansion section. Values of α_b also ranged from 3 to 10 in both cases.

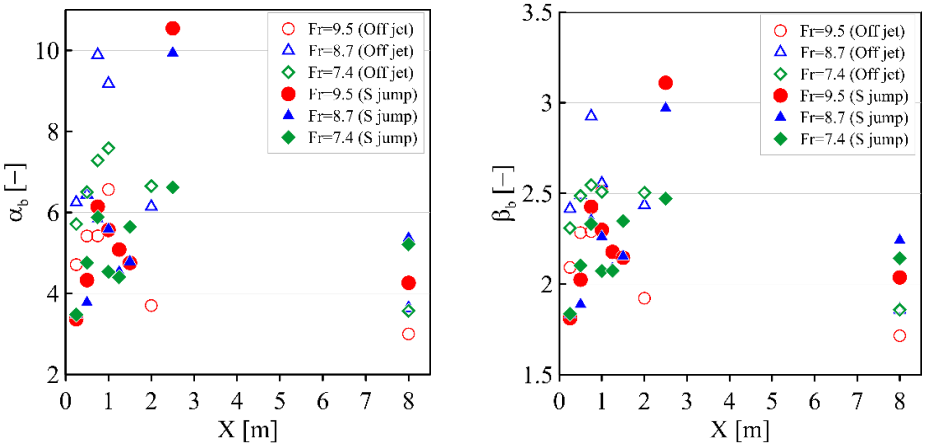

Figure 3. Values βb and αb calculated in measuring sections for asymmetric S-type jump and the position of the jet system in the flow path (in the off state)

The values of α_b and β_b using the water jet injection system under the tested tailwater conditions for each configuration and in the measurement section located 0.5 m after the system are given in Table 1. They were comparing the results with the initial values given in Fig. 3 shows that in all the different configurations of the water jet injection system, β_b has been reduced to less than 1.46. The maximum α_b values are less than two except in one configuration. These results confirm the effectiveness of the system in flow stabilization and homogenization.

Table 1. Results of α_b and β_b calculated using water jet injection system in different configurations.

Configuration	P= 0.4 (m)		P= 0.6 (m)		P= 0.8 (m)	
	β_b	α_b	β_b	α_b	β_b	α_b
Fr=7.4						
Q jet= 0.0081 (m^3/s), n=9	1.02	1.06	1.18	1.57	1.35	2.07
Q jet= 0.0072 (m^3/s), n=9	1.23	1.69	1.26	1.72	1.2	1.56
Q jet= 0.0081 (m^3/s), n=7	1.10	1.29	1.22	1.64	1.18	1.53
Q jet= 0.0072 (m^3/s), n=7	1.03	1.09	1.13	1.40	1.18	1.53
Q jet= 0.0081 (m^3/s), n=5	1.46	2.48	1.04	1.12	1.11	1.32
Q jet= 0.0072 (m^3/s), n=5	1.26	1.82	1.01	1.04	1.07	1.22
Fr=8.7						
Q jet= 0.0081 (m^3/s), n=9	1.03	1.10	1.31	1.93	1.36	2.05
Q jet= 0.0072 (m^3/s), n=9	1.02	1.07	1.07	1.21	1.13	1.44
Q jet= 0.0081 (m^3/s), n=7	1.09	1.24	1.18	1.51	1.27	1.80
Q jet= 0.0072 (m^3/s), n=7	1.05	1.14	1.16	1.46	1.15	1.46
Q jet= 0.0081 (m^3/s), n=5	1.28	1.85	1.11	1.33	1.23	1.66
Q jet= 0.0072 (m^3/s), n=5	1.13	1.40	1.07	1.21	1.07	1.22
Fr=9.5						
Q jet= 0.0081 (m^3/s), n=9	1.04	1.13	1.22	1.63	1.35	2.02
Q jet= 0.0072 (m^3/s), n=9	1.05	1.14	1.14	1.40	1.2	1.60

Configuration	P= 0.4 (m)		P= 0.6 (m)		P= 0.8 (m)	
	β_b	α_b	β_b	α_b	β_b	α_b
Q jet= 0.0081 (m^3/s), n=7	1.07	1.20	1.1	1.28	1.19	1.57
Q jet= 0.0072 (m^3/s), n=7	1.04	1.12	1.08	1.23	1.14	1.42
Q jet= 0.0081 (m^3/s), n=5	1.18	1.51	1.08	1.23	1.18	1.55
Q jet= 0.0072 (m^3/s), n=5	1.1	1.28	1.03	1.09	1.08	1.24

Fig. 4 shows a schematic diagram of the hydraulic performance of the jet injection system in interaction with the S-type jump in the expansion channel.

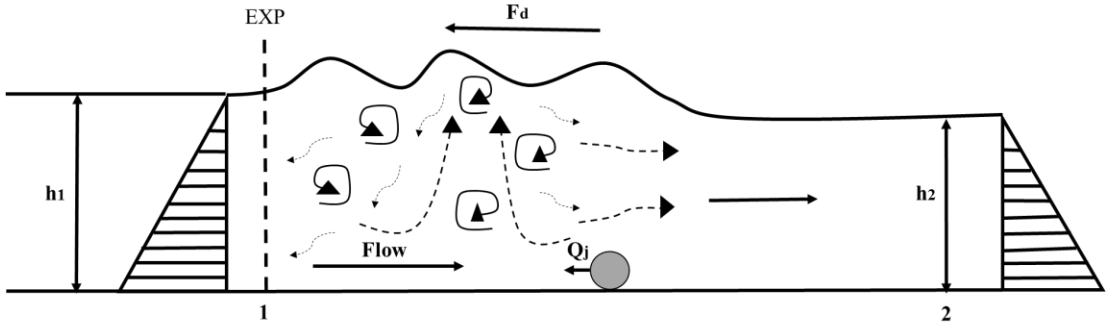

Figure 4- Definition sketch for application of momentum equation

The momentum equation according to Equation 5, assuming the distribution of hydrostatic pressure and ignoring the shear stress of the bed, was used between sections 1 and 2 (Fig. 4):

$$F_d = (P_1 + M_1) - (P_2 + M_2) = S_1 - S_2 \quad (5)$$

Where the drag force F_d can be expressed as the difference between the sum of the pressure force ($P_i = ½ \rho g y_i^2$) and the momentum flux ($M_i = \beta_i \cdot \rho \cdot Q \cdot v_i$).

Q: volumetric flow rate; v_i: flow velocities at the two ends of the jump; ρ: water density; g: gravitational acceleration; β_i: momentum correction coefficient; y_i: flow depth.

Section 1 is considered at the end of the expansion section and section 2 is 0.5 m downstream of the jet injection system.

The dimensional form of the drag force according to Equation 6 is considered in the experimental interpretation of the results:

$$C_{Fd} = 1 - \frac{S_2}{S_1} \quad (6)$$

Fig. 5 indicates the observed C_{Fd} values and water depth ratio h_1 / h_2 for different variables considered in the tested configurations: distance of the jet system from the abrupt expansion cross-section in the flume, number of holes of water jet injection system and jet flow, under the three considered hydraulic condition (Fr).

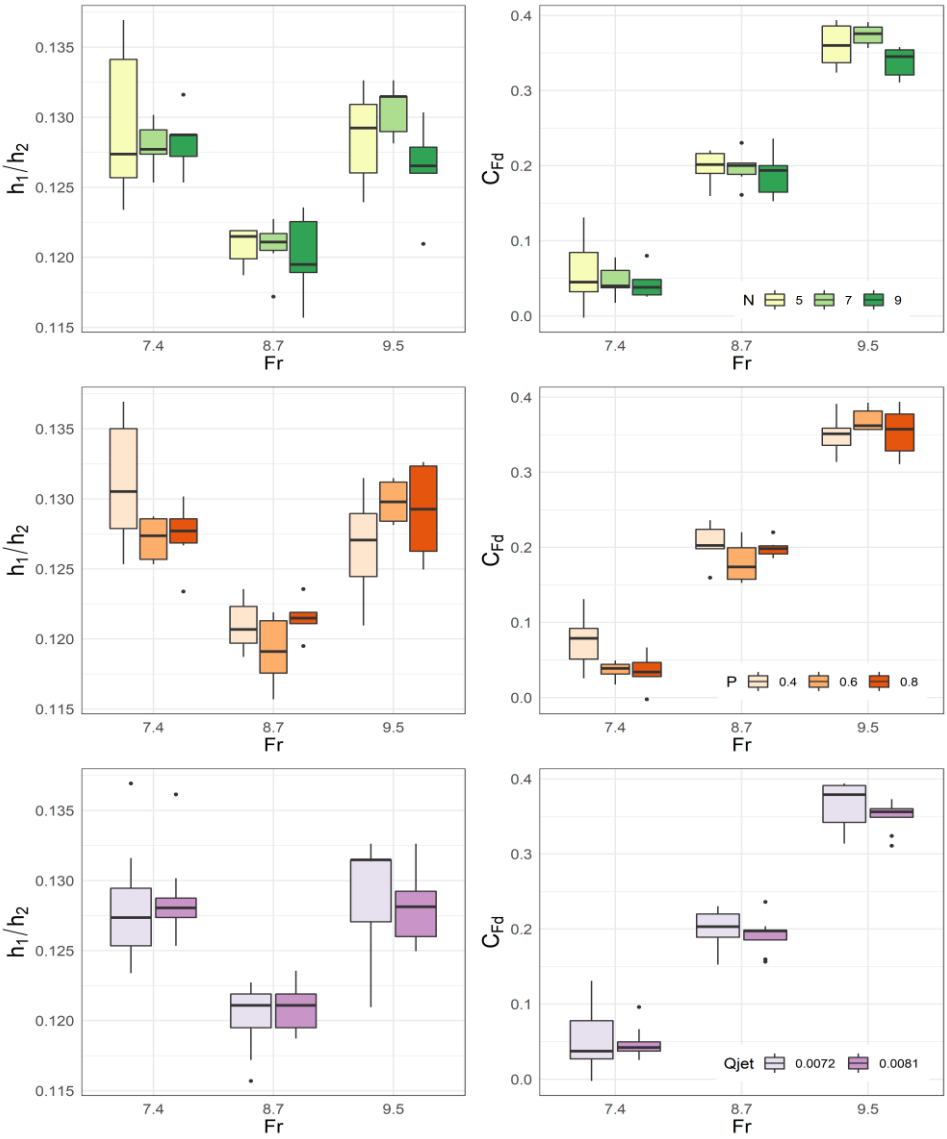

Figure 5. Experimental values of C_{Fd} and h_1/h_2 for tested hydraulic conditions

h_1/ h_2 values vary from 0.116 to 0.137. The minimum values of h_1/ h_2 correspond to the Fr=8.7, which indicates more tailwater and higher immersion. The results for C_{Fd} (from 0 to 0.394, with an average of 0.2) show the good performance of the water jet injection system and the downstream flow uniformity in all the tested configurations. The maximum C_{Fd} is for P= 0.4 m. Compared to 0.6 and 0.8 meters at this distance, the jets interact with the inlet flow at a shorter distance. As a result, it creates more turbulence in the expansion section, and more energy is wasted in this area. As a result, P equals 0.4 m, creating less S_2 (total pressure force and momentum flux) in the tailwater. Fig. 5 also shows that the minimum drag force was observed at Fr = 7.4 for N= 5, with a higher h_1/ h_2. In this case, water jets are injected more rapidly into the inlet flow. As a result, the total momentum increases in the expansion cross section. Increasing the effective depth of the inlet flow, breaking the flow, turbulence and

vortices created cause energy dissipation and reduce the jump length in downstream of the system. Increasing the jet flow increases the momentum in the expansion section and thus reduces the drag force downstream of the system, which is also clearly seen in Fig. 5.
Among the different configurations tested, the three configurations presented in Table 2, which had lower α_b and β_b , were selected to analyze the stable performances of the dissipator under variable downstream conditions that may occur under operating conditions.

Table 2. Characteristics of the selected configurations of the jet system

Configuration	Fr	Q_j (m^3/s)	n	P (m)
1	7.4	0.0072	7	**0.4**
2		0.0081	9	**0.4**
3		0.0072	5	**0.6**

The different percentages of the tailwater depths considered to determine the variable downstream conditions are described as follows:

- The end gate of the flume is fully open, as it has no effect on the tailwater depth. This scenario was considered to investigate the performance and impact of the dissipator without any control over the tailwater depth (0.55hs, 0.65hs, and 0.75hs percentages for Froude numbers 7.4, 8.7 and 9.5, respectively).
- To investigate the performance of the dissipator under conditions of shallower tailwater depth, the impact of the end gate of the flume and the formation of tailwater depths shallower than that required for the formation of S-jumps are considered. For all three optimal configurations, this scenario first considered the case with the shallowest tailwater depth that can be formed by pulling down the gate. Then, several other cases with a tailwater depth greater than this value and less than the tailwater depth required to form S-jumps were tested. (0.75hs, 0.8hs and 0.9hs percentages)
- A tailwater depth is formed which is greater than the depth required to form the S-jump. This case also investigated the system performance in conditions like a flood, where a greater tailwater depth is formed (1.2 hs percentages for all three Froude numbers tested).
- The coefficients α_b and β_b calculated along the flume for different tailwater percentages are shown in the three optimal configurations mentioned in Fig. 6 to 8.

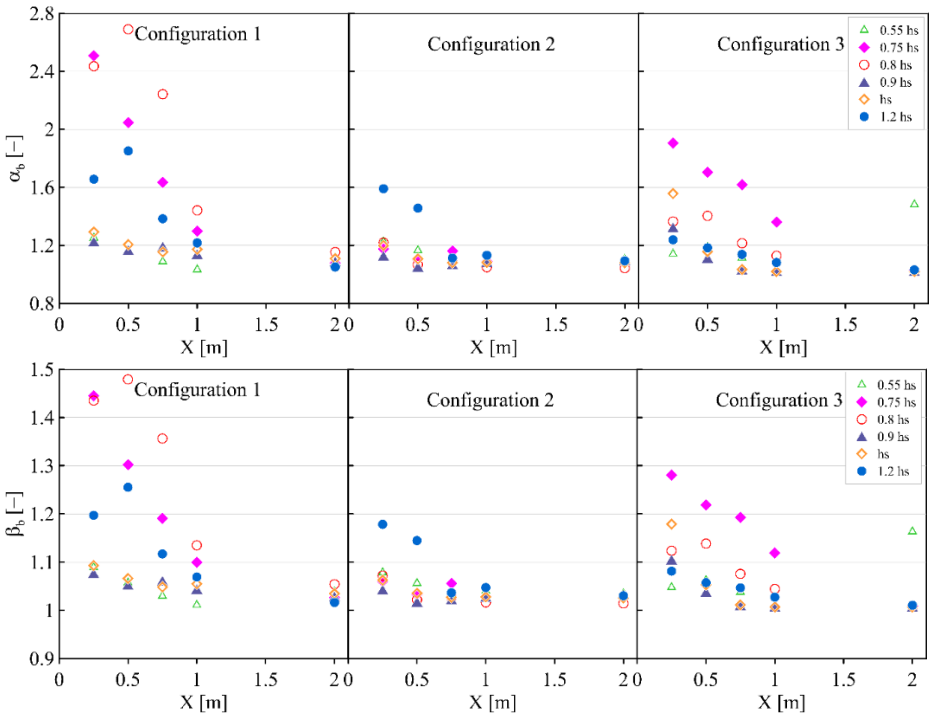

Figure 6. Values α_b and β_b calculated in measuring sections under different tailwater depths for the three optimal configurations (Fr= 7.4)

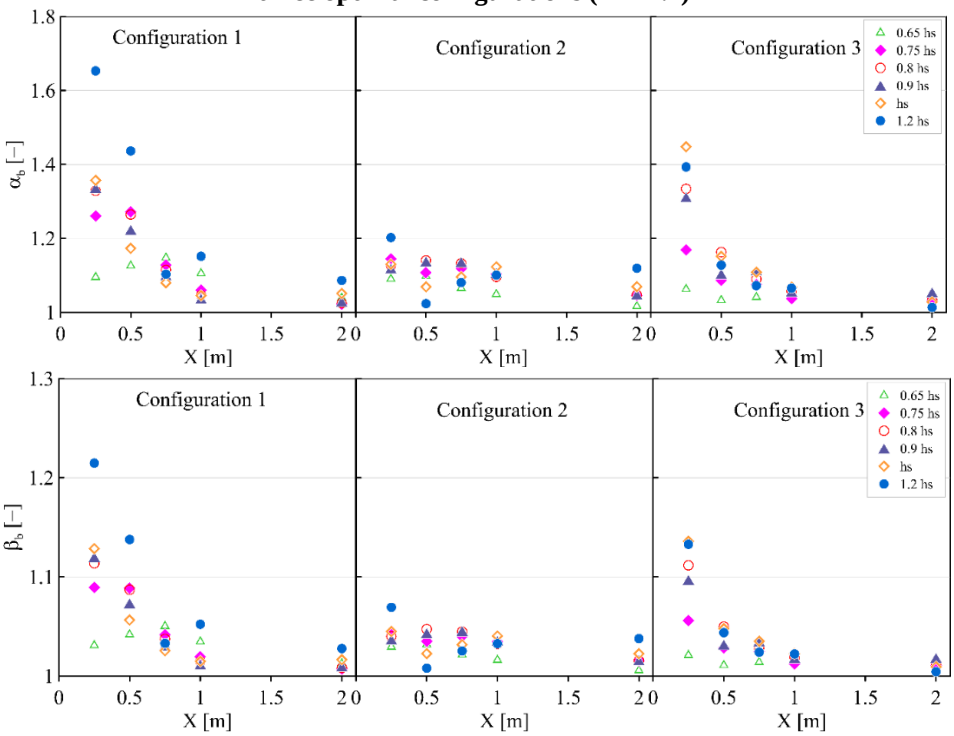

Figure 7. Values α_b and β_b calculated in measuring sections under different tailwater depths for the three optimal configurations (Fr= 8.7)

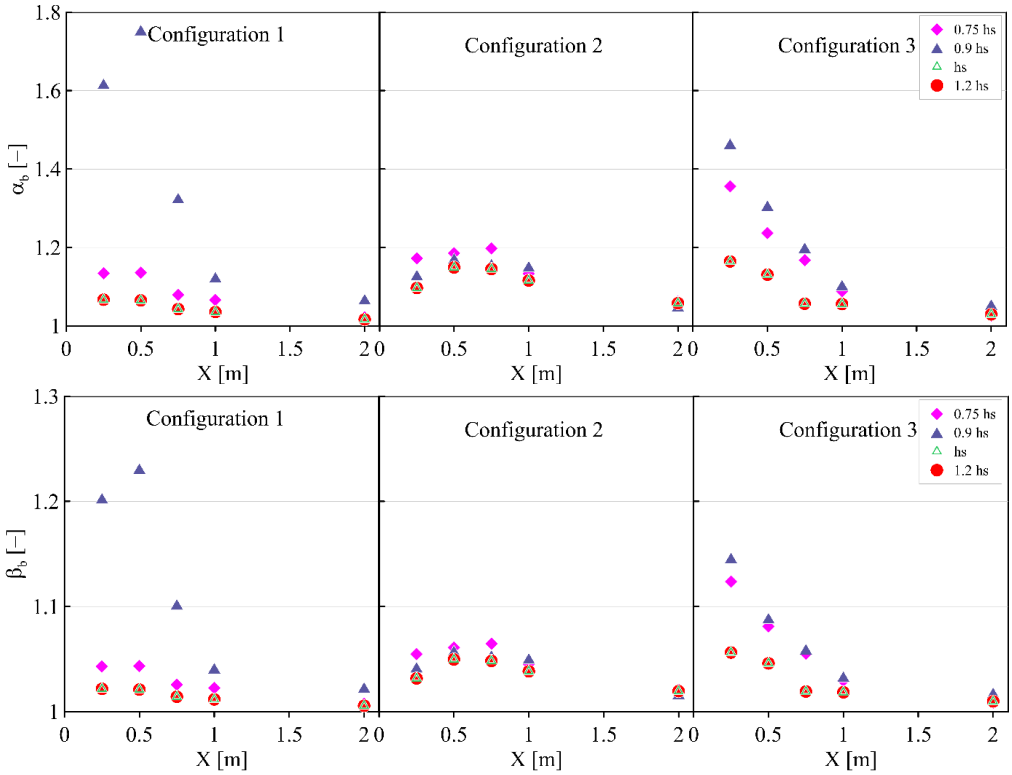

Figure 8. Values α_b and β_b calculated in measuring sections under different tailwater depths for the three optimal configurations (Fr= 9.5)

Fig. 6 to 8 show information about the efficiency of the three optimal configurations at the 0.25, 0.5, 0.75, 1 and 2 m downstream cross-sections of the water jet injection system and the tested variable flow conditions. Although different values appear for each configuration, the qualitative trends α_b and β_b are very similar. As shown in Fig. 6 to 8, the use of a water jet injection system has significantly improved flow status even at low tailwater levels. The values of α_b and β_b in all measured sections were much lower than those observed in the initial S-jump mode in the measured sections. In practical terms, this means that using this water jet injection system eliminates the hydraulic instabilities of the S-jump and reduces the length of the stilling basin. All three optimal tested configurations in this study have good and almost identical results. But as can be seen, the amount of α_b and β_b in optimal configuration 2 is lower than in configurations 1 and 3. Also, the different tested percentages in configuration 2 are less different. In this configuration, the injected water jet is more than the other two configurations. This higher injection jet rate (Qj = 0.0081 m3/s) generates more energy in contact with the incoming flow jet of the channel. As a result of this contact, more energy is consumed in that area (before the jet system), and less energy is transferred to the after of the jet system. Finally, the sections after the jet system, especially the sections 0.25 and 0.5 m after the jet, have less turbulence and kinetic energy than the same sections in the other two configurations. Configuration 2 has nine water injection jets (n), while configurations 1 and 3 have 7 and 5 jets, respectively. This number of more water injection jets in this configuration helps to distribute more inlet flow jets evenly. As a result, the flow after the jet system is distributed more evenly in the sections and reduces energy. Also, the jet injection (P) distance in configuration 2 is equal to 40 cm, while this distance in configuration 3 is equal to 60 cm. This distance also causes the water injection jet to

collide closer to the flow inlet jet. As a result, more energy is consumed, and the values of αb and βb decrease after the jet system. The results of βb and αb show that with increasing distance due to increased energy dissipation, distance from the jump and the injection site of the jet increases, the situation tends to be uniform. The results show that in the three tested Froude numbers at different depths, the uniformity coefficient in sections 0.25 to 0.75 m is slightly higher than sections 1 and 2 m. From section 1m onwards, the coefficients tend to be a fixed routine in all conditions, and the depth of the tailwater will not affect changes in velocity and energy. It is probably because the jet generates a counter flow. Both inlet and jet flows are opposite, there is so much mixing and surface rolls in the jet area that it does not reach after the jet and damp each other there, and resonance does not occur. At Froude number equal to 9.5, a 20% increase in the tailwater depth has the same results as the main tailwater, indicating that the system can operate properly even in the event of a flood. Another point that can be seen in the figures is that when the tailwater depth is not affected by the gate and the gate is fully open, the coefficients αb and βb have small values. That indicates the good performance of the water jet injection system in hydraulic jump stability and flows uniformity in abruptly expanding channels.

Fig. 9 shows the kinetic energy correction coefficients (α) and momentum (β) calculated on the total cross-section according to equations (3) and (4), for three optimal configurations with four different tailwater depths (0.75hs, 0.8hs, 0.9hs, hs) in the downstream of the jet system.

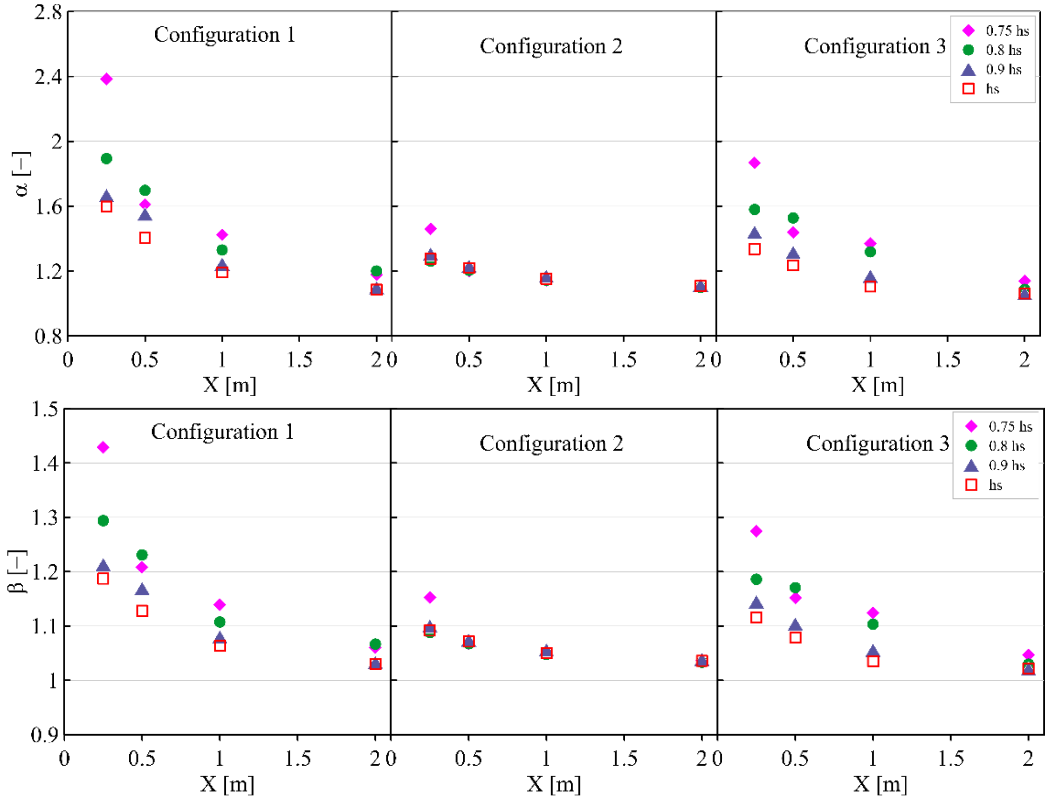

Figure 9. Values α and β were calculated in measuring sections under different tailwater depths for the three optimal configurations (Fr= 7.4)

In general, Fig. 9 shows that as the distance increases and moves downstream of the channel, the values of α and β decrease, and the current gradually becomes uniform. In all three tested configurations at different sections and tailwater depths, α values range from 1.06 to 2.39, and β values range from 1.02 to 1.43. These results show that the values of α and β have a significant decrease compared to the results obtained in the asymmetric S-type jump, which indicates the good performance of the water jet injection system in the stability of the asymmetric jump. The highest values of α and β were observed in configuration one and in the 0.75hs tailwater with a cross-section of 0.25 m. The flow reaches a uniformity in the cross-section of 1 m and later in three configurations and for the tested different tailwater depths. Configuration 2 is also stable for lower tailwater depths, indicating the system's ability to stabilize asymmetric jumps even with less force downstream. These results confirm the results of Fig. 6 to 8.

One of the most important issues that can be investigated in the study of the effectiveness of water jet injection systems in the stability of asymmetric jumps in expanding channels is the study of the relative energy loss in the hydraulic jump in the use of water jet injection systems. If E_1 and E_2 represent the specific energy at the beginning and end of the jump, respectively, and E_L represents the amount of energy loss in the jump, using the energy equation in sections 1 and 2, we have:

$$E_L = E_1 - E_2 = (y_1 + \frac{V_1^2}{2g}) - (y_2 + \frac{V_2^2}{2g}) \quad (7)$$

The ratio of energy loss to initial energy of hydraulic jump is called the relative energy loss of hydraulic jump, which is defined as follows:

$$\eta = \frac{E_L}{E_1} = \frac{E_1 - E_2}{E_1} \quad (8)$$

By measuring the average depth velocity and using equation 8, the relative energy loss values in the asymmetric jump of S-type in the expanding channel for the initial Froude numbers 7.4, 8.7, and 9.5 are presented in Fig. 10. Section 1 at the end of the expanding section (beginning of the jump) and section 2 in the measurement sections considered after the expanding section (X= 0.25, 0.5, 0.75, 1, 1.25, 1.5, 1.75, 2, 3, 4, 6 and 8 meters) is considered. X_{EXP} is also the expansion length, which is equal to 0.6 meters.

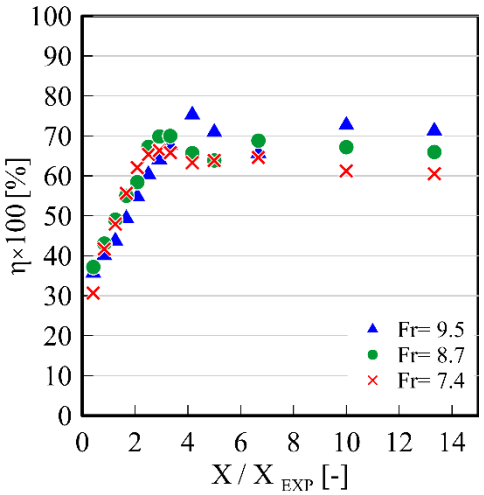

Figure 10. Relative energy loss values in S-type asymmetric jump in expanding channel for initial Froude numbers 7.4, 8.7 and 9.5

As can be seen in Fig. 10, the trend of changes in relative energy loss is such that as the Froude number increases, the relative energy loss also increases. In the tested Froude numbers, the lowest relative energy loss occurred at Froude number 7.4 and the highest at Froude number 9.5. According to Alhamid [26], the relative energy loss in S-type asymmetric jump for different expanding ratios is a function of the Froude number in horizontal and sloping beds. The results in Fig. 10 confirm the results of Alhamid [26]. The relative energy loss in the tested Froude numbers up to X / X_{EXP} =2.5 after the expanding section has an increasing trend and reaches its maximum value at X / X_{EXP} = 4 and extends to the tailwater with a constant almost linear trend. Fig. 11 shows the relative energy loss in the use of water jet injection system in the stability of S-type asymmetric jump in the expanding channel for three optimal configurations at the tailwater depths 0.75hs, 0.8hs, 0.9hs and hs with a Froude number 7.4. E_1 and E_2 represent the specific energy before and after the water jet injection system, respectively. Here, section 1 at the end of the expanding section (before the water jet injection system) and section 2 in the measurement sections considered after the water jet injection system (X =0.25, 0.5, 1 and 2 meters) has been.

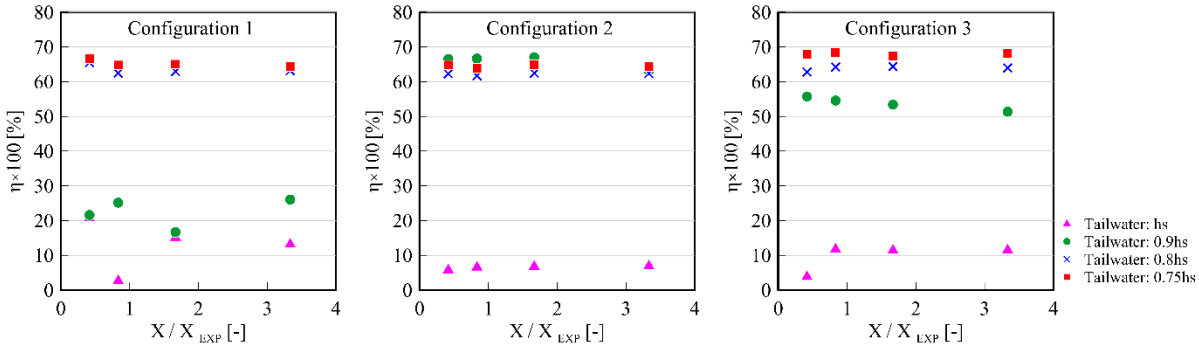

Figure 11. Relative energy loss in using water jet injection system for three optimal configurations with different tailwater depths (Fr= 7.4)

As can be seen in Fig. 11, the average relative energy loss in configuration one at 0.25, 0.5, 1, and 2 m sections for the tailwaters of 0.75hs, 0.8hs, 0.9hs, and hs is 65.19, 63.5, 22.37, and 12.92 %, respectively. These values are 64.45, 62.18, 65.83 and 6.49 % for configuration 2 and 67.96, 63.82, 53.75 and 9.63 % for configuration 3 respectively. The results of Fig. 11 show that the tailwater of hs in all three optimal configurations and the tailwater of 0.9hs in configuration 1 have lower relative energy loss values than other tailwater depths, which is due to the higher water depth in the expansion section. Increasing the initial depth caused by increasing the tailwater depth causes more energy loss at the same expansion section, and less energy is transferred downstream. So that the relative energy loss of the hs tailwater compared to the energy loss in the expansion cross-section of S-type jump (initial depth of S-type jump) is equal to 54.14, 57.15, and 54.76 % for configurations 1, 2, and 3, respectively. Also, it is equal to 48.5 % in the 0.9hs of tailwater for configuration 1.

For this reason, after the jet injection system, the flow becomes more uniform and the length of the stilling basin decreases. According to the research of Neisi and Shafai Bajestan [27], the relative energy loss is a function of the initial Froude number and cross-sectional opening ratio. At a constant opening ratio, the S-jump efficiency with a rough bed is higher than the S-jump with a smooth bed. The results obtained from the use of a water jet injection system in the stability of asymmetric jumps in this study confirm the results of Neisi and Shafai Bajestan [27].

In general, the results show that in the water jet injection system, eddy currents resulting from the collision of the water jet with the inlet flow increase the shear stress of the bed and as a result, the supercritical flow energy is more consumed. In addition to the increase of relative energy loss in the jump and decrease in the erosive power of the outlet flow from the stilling basin, this system has a significant effect on the flow pattern in the hydraulic jump. So that the injection of water jets causes the transfer of the end rollers of the hydraulic jump from the bottom of the basin to the upper parts and the surface of the water, which can also be effective in reducing the erosive power of the outlet flow of the basin and reducing the required diameter of rip rap at the end of the stilling basin.

There are consecutive and unstable waves in S-jump that move over time and return to the first place after a few seconds. The displacement of these waves relative to the expansion section and the S-jump length for the tested Froude numbers is shown in the Fig. 12.

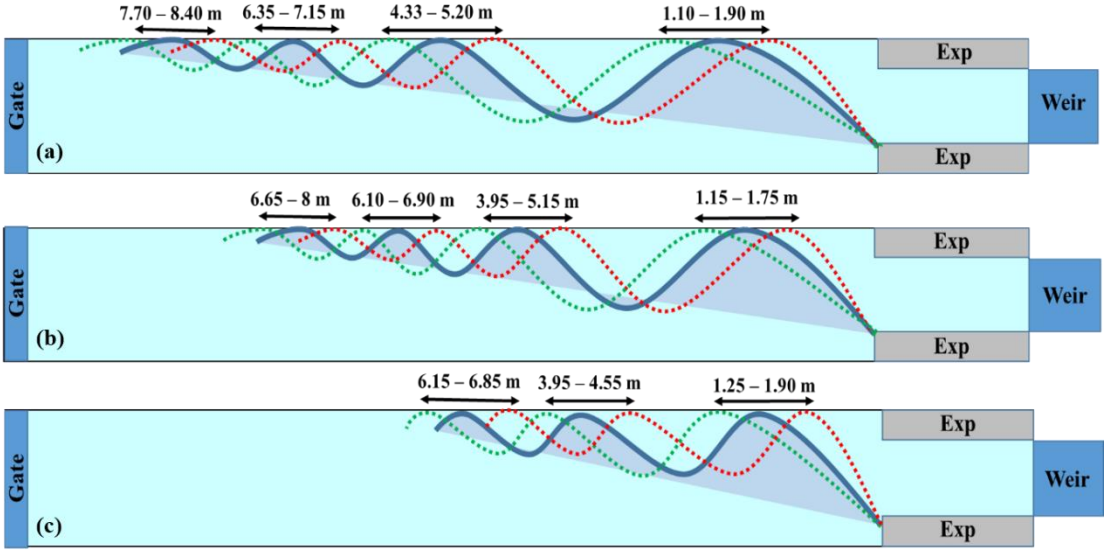

Figure 12- The S-jump length and displacement rate of consecutive and unstable waves for the tested Froude numbers; (a) Fr = 7.4 (b) Fr = 8.7 (c) Fr = 9.5

As shown in the Fig.12, the S-jump length for Froude numbers 7.4, 8.7, and 9.5 is 8.4, 8 and 6.85m, respectively. The displacement average of consecutive and unstable waves created in these jumps is 0.79, 0.99, and 0.65m (for Froude numbers 7.4, 8.7, and 9.5, respectively). It should be noted that the jump length is equal to the distance from the start of the jump to a point on the water surface immediately after the last rolling wave, in which case the height of this point is approximately equal to the height of the tailwater.

By using the water jet injection system, consecutive and unstable waves are eliminated. Rolling waves on the water surface also end shortly after the system. Fig. 13 shows the ratio of jump length to tailwater depth to the corresponding Froude numbers for the tested different configurations and S-jump. The results show the effectiveness of the water jet injection system well.

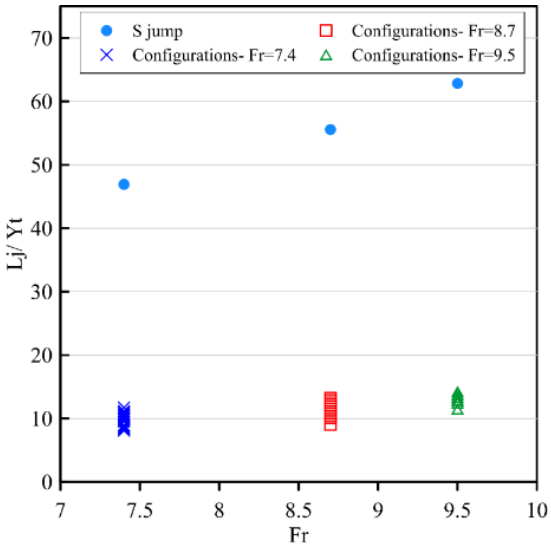

Figure 13 - Ratio of jump length to tailwater depth versus Froude numbers for the tested different configurations and S-jump

In this research, the percentage of reduction of hydraulic jump length by using water jet injection system has been calculated according to Equation (9):

$$T = \frac{L_{j_{(S-jump)}} - L_j}{L_{j_{(S-jump)}}} \times 100 \tag{9}$$

In this equation, $L_{j(S\text{-}jump)}$ is S-jump length and L_j is hydraulic jump length using water jet injection system in the same Froude numbers. Fig. 14 shows the variation of T values for the three optimal configurations at different tailwater depths.

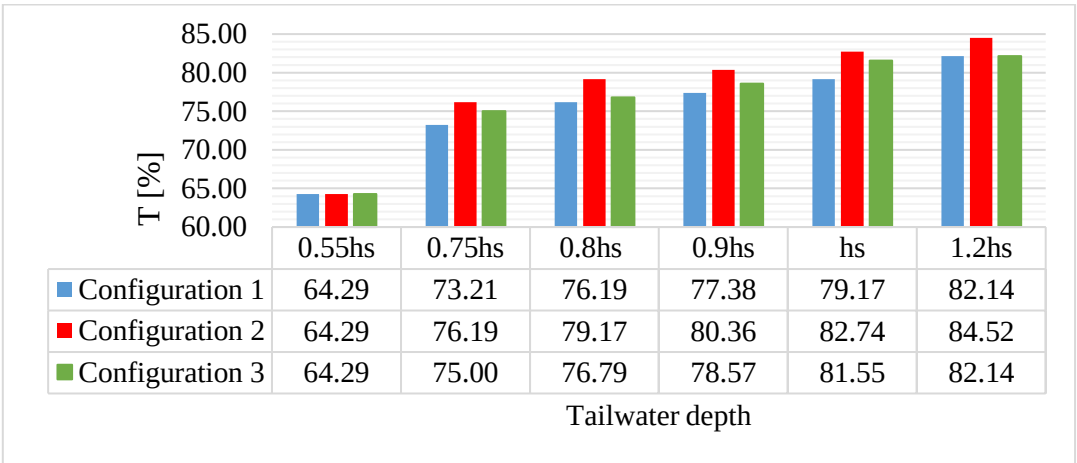

	0.55hs	0.75hs	0.8hs	0.9hs	hs	1.2hs
Configuration 1	64.29	73.21	76.19	77.38	79.17	82.14
Configuration 2	64.29	76.19	79.17	80.36	82.74	84.52
Configuration 3	64.29	75.00	76.79	78.57	81.55	82.14

Figure 14 - Variation of T values for three optimal configurations at different tailwater depths

As can be seen in Fig. 14, the reduction in hydraulic jump length has also increased with increasing tailwater depth. The configurations 1, 2 and 3 for the hs tailwater depth show 79.17, 82.74, and 81.55% reduction in the S-jump length, respectively. The percentage of jump length reduction in configuration 2 is higher than 1 and 3. In general, the results show that the use of

water jet injection system causes stability and elimination of asymmetric S-jump waves and significantly reduces the jump length.

4. Conclusions

In this experimental study, the flow properties in interaction with the water jet injection system and the asymmetric S-type jump have been investigated. For this purpose, 54 different configurations of water jet injection systems were tested, and their relative performance in terms of flow uniformity and average longitudinal velocity of the system downstream was discussed through two parameters energy and momentum correction coefficients. The results showed a significant reduction of these parameters in all system configurations. For the three configurations with lover energy and momentum correction coefficients, the performance stability under lower tailwater conditions was evaluated by assessing the flow properties downstream from the device. The results showed that the values of energy and momentum correction coefficients for the tested configurations decrease by moving in the downstream direction and increasing the tailwater depth. As a result, in all tailwater depths from 1 m section onwards, not many changes in the flow properties were observed. Configuration 2 showed more uniform values and higher energy dissipation than configurations 1 and 3. Also, a water jet injection system showed a significant relative energy loss in the asymmetric S-jump. The highest relative energy loss was observed in the different tested sections and tailwater depths equal to 66.66, 67.02, and 68.42 % for configurations 1, 2, and 3. The jump lengths for the mentioned optimal configurations in the hs tailwater depth showed a decrease of 79.17, 82.74, and 81.55%, respectively. In general, the presented experimental study showed that the interaction of the water jet injection system with hydraulic jump causes stabilization, jump stability, and flow uniformity control by breaking the main flow and redistributing the velocity field in the stilling basin. Also, using this method, the basin's length, which is one of the important factors in designing a stilling basin, is reduced.

Acknowledgments

We are grateful to the Research Council of Shahid Chamran University of Ahvaz for financial support.

References

1. Chow, V(1959)Open-channel hydraulics, McGraw-Hill, New York.
2. Tharp, EL(1966)Modification of the hydraulic jump by submerged jets.
3. Rajaratnam, N(1964)The forced hydraulic jumpWater Power, 16(2), 14-19.
4. Basco, DR., & Adams, JR(1971)Drag forces on baffle blocks in hydraulic jumpsJournal of the Hydraulics Division. 2035-2023,(12)97.
5. Rajaratnam, N., & Murahari, V(1971)A contribution to forced hydraulic jumpsJournal of Hydraulic Research, 9(2), 217-240.
6. Peterka, AJ(1974)Hydraulic design of stilling basins and energy dissipatorsUnited States Department of the Interior, Bureau of Reclamation.
7. Ohtsu, I., Yasuda, Y., & Yamanaka, Y(1991)Drag on vertical sill of forced jumpJournal of Hydraulic Research, 29(1), 29-47.
8. Hager, WH(1992)Energy dissipators and hydraulic jump, Kluwer Academic, Dordrecht, Netherlands.
9. Thompson, PL., & Kilgore, RT(2006)Hydraulic Design of Energy Dissipators for Culverts and Channels: Hydraulic Engineering Circular Number 14 (NoFHWA-NHI-06-086)National Highway Institute (US).

10. Habibzadeh, A., Wu, S., Ade, F., Rajaratnam, N., & Loewen, MR(2011)Exploratory study of submerged hydraulic jumps with blocksJournal of Hydraulic Engineering, 137(6), 706-710.
11. Abdelhaleem, FSF(2013)Effect of semi-circular baffle blocks on local scour downstream clear-overfall weirsAin Shams Engineering Journal, 4(4), 675-684.
12. Aal, GMA., Sobeah, M., Helal, E., & El-Fooly, M(2018)Improving energy dissipation on stepped spillways using breakersAin Shams Engineering Journal, 9(4), 1887-1896.
13. Herbrand, K(1973)The spatial hydraulic jumpJournal of Hydraulic Research, 11(3), 205-218.
14. Scorzini, AR., Di Bacco, M., & Leopardi, M(2016)Experimental investigation on a system of crossbeams as energy dissipator in abruptly expanding channelsJournal of Hydraulic Engineering, 142(2), 06015018.
15. Bremen, R., and Hager, WH(1993)T-jump in abruptly expanding channelJHydraulRes., 31(1), 61–78.
16. Varol, F., Cevik, E., & Yuksel, Y(2009)The effect of water jet on the hydraulic jumpIn Thirteenth International Water Technology Conference, IWTC (Vol13, pp895-910).
17. Wali, UG(2013)Kinetic energy and momentum correction coefficients for a small irrigation channelInternational Journal of Emerging Technology and Advanced Engineering, 3(9), 1-8.
18. Khalili Shayan, H ., &Farhoudi, J(2013)Theoretical criterion for stability of free hydraulic jump on adverse stilling basinsJournal of Hydraulic Structures, 1(2), 53-66.
19. Helal, E., Abdelhaleem, FS., & Elshenawy, WA(2020)Numerical Assessment of the Performance of Bed Water Jets in Submerged Hydraulic JumpsJournal of Irrigation and Drainage Engineering, 146(7), 04020014.
20. Hajialigol, S., Ahadiyan, J., Sajjadi, M., Rita Scorzini, A., Di Bacco, M., & Shafai Bejestan, M(2021)Cross-Beam Dissipators in Abruptly Expanding Channels: Experimental Analysis of Flow PatternsJournal of Irrigation and Drainage Engineering, 147(11), 06021012.
21. Sharoonizadeh S, Ahadiyan J, Scorzini AR, Di Bacco M, Sajjadi M, Moghadam MFExperimental Analysis on the Use of Counterflow Jets as a System for the Stabilization of the Spatial Hydraulic JumpWater2021; 13(18):2572https://doi.org/10.3390/w13182572.
22. Mohanty, PK., Dash, SS., Khatua, KK., & Patra, KC(2012)Energy and momentum coefficients for Wide compound channelsRiver Basin Management VII, 172, 87.
23. Seckin, G., Ardiclioglu, M., Cagatay, H., Cobaner, M., & Yurtal, R(2009)Experimental investigation of kinetic energy and momentum correction coefficients in open channelsScientific Research and Essays, 4(5), 473-478.
24. Hamidifar, H., Omid, MH., & Keshavarzi, A(2016)Kinetic energy and momentum correction coefficients in straight compound channels with vegetated floodplainJournal of Hydrology, 537, 10-17.
25. Keshavarzi, A., & Hamidifar, H(2018)Kinetic energy and momentum correction coefficients in compound open channelsNatural Hazards, 92(3), 1859-1869.
26. Alhamid, AA(2004)S-jump characteristics on sloping basinsJournal of Hydraulic research, 42(6), 657-662.
27. Neisi, K., & Shafai Bejestan, M(2013)Characteristics of S-jump on roughened bed stilling basinJournal of Water Sciences Research, 5(2), 25-34.